Applied Geochemistry 87 (2017) 146–157

Contents lists available at ScienceDirect

Applied Geochemistry

journal homepage: www.elsevier.com/locate/apgeochem

Geochemistry and speciation of Fe(II) and Fe(III) in natural geothermal water, Iceland

Hanna Kaasalainen[a,b,*], Andri Stefánsson[a], Gregory K. Druschel[c]

[a] Institute of Earth Sciences, Science Institute, University of Iceland, Askja, Sturlugata 7, 101 Reykjavik, Iceland
[b] Applied Geochemistry, Department of Civil, Environmental and Natural Resources Engineering, Luleå University of Technology, 971 87 Luleå, Sweden
[c] Department of Earth Sciences, Indiana University-Purdue University Indianapolis, Indianapolis, IN 46202, USA

ARTICLE INFO

Handling Editor: H. Armannsson

Keywords:
Iron
Redox speciation
Natural water
Geothermal water
Nanoparticulate Fe

ABSTRACT

The geochemistry of Fe(II) and Fe(III) was studied in natural geothermal waters in Iceland. Samples of surface and spring water and sub-boiling geothermal well water were collected and analyzed for Fe(II), Fe(III) and Fe_{total} concentrations. The samples had discharge temperatures in the range 27–99 °C, pH between 2.46 and 9.77 and total dissolved solids 155–1090 mg/L. The concentrations of Fe(II) and Fe(III) were determined in the < 0.2 μm filtered and acidified fraction using a field-deployed ion chromatography spectrophotometry (IC-Vis) method within minutes to a few hours of sampling in order to prevent post-sampling changes. The concentrations of Fe (II) and Fe(III) were < 0.1–130 μmoL/L and < 0.2–42 μmoL/L, respectively. In-situ dialysis coupled with Fe(II) and Fe(III) determinations suggest that in some cases a significant fraction of Fe passing the standard < 0.2 μm filtration method may be present in colloidal/particulate form. Therefore, such filter size may not truly represent the dissolved fraction of Fe but also nano-sized particles. The Fe(II) and Fe(III) speciation and Fe_{total} concentrations are largely influenced by the water pH, which in turn reflects the water type formed through various processes. In water having pH of ~7–9, the total Fe concentrations were < 2 μmoL/L with Fe(III) predominating. With decreasing pH, the total Fe concentrations increased with Fe(II) becoming increasingly important and predominating at pH < 3. In particular in waters having pH ~6 and above, iron redox equilibrium may be approached with Fe(II) and Fe(III) possibly being controlled by equilibrium with respect to Fe minerals. In many acid waters, the Fe(II) and Fe(III) distribution may not have reached equilibrium and be controlled by the source(s), reaction kinetics or microbial reactions.

1. Introduction

Iron is an important redox-active element in geothermal water and its chemistry and speciation are of both scientific and environmental interest due to its role in mineral dissolution and precipitation reactions, metal(loid) sequestration, and biogeochemical processes related to thermophilic ecosystems (e.g. Stefánsson et al., 2001, 2005; Nordstrom et al., 2005; Shock et al., 2010; Kaasalainen and Stefánsson, 2012). Iron is present in water as ferrous (Fe(II)) and ferric (Fe(III)) iron, may complex with inorganic or organic ligands, and also form polymers, nanoparticulate colloidal aggregates, and crystalline Fe minerals (e.g. Stumm and Morgan, 1981; Stumm and Sulzberger, 1992; Rue and Bruland, 1995; Banfield and Navrotsky, 2001; Cornell and Schwertmann, 2003; Gilbert et al., 2007; Hiemstra, 2015). The speciation and transformations between the solid and soluble Fe species occur over the entire redox range of water, depend on factors such as pH, temperature, and organic complexation, and may be kinetically controlled and photochemically induced (Stumm and Morgan, 1981; Stumm and Sulzberger, 1992).

Dissolved iron concentrations in surface geothermal waters range from < 1 μg/L to several hundreds of mg/L, as conventionally determined in samples filtered through 0.1–0.45 μm pore size followed by acidification (e.g. Gunnlaugsson and Arnórsson, 1982; Stefánsson et al., 2001, 2005; Nordstrom et al., 2005; McCleskey et al., 2014; Kaasalainen and Stefánsson, 2012; Pope and Brown, 2014). Iron concentrations typically show distinct trends with pH, and Fe varies from being present at trace concentrations in waters having alkaline to circum-neutral pH to being one of the major elements in acid water. Concentrations of Fe(II) and Fe(III) are not routinely analyzed in geothermal water, and thus some uncertainty remains on the typical Fe(II) and Fe(III) concentrations and the main processes controlling their concentration in geothermal water. Based on the existing data and the results of thermodynamic calculations it is evident that the absolute and relative Fe(II) and Fe(III) concentrations vary significantly (Heinrich

* Corresponding author. Applied Geochemistry, Department of Civil, Environmental and Natural Resources Engineering, Luleå University of Technology, 971 87 Luleå, Sweden.
E-mail address: hanna.kaasalainen@ltu.se (H. Kaasalainen).

http://dx.doi.org/10.1016/j.apgeochem.2017.10.021
Received 28 April 2017; Received in revised form 24 October 2017; Accepted 25 October 2017
Available online 26 October 2017
0883-2927/

and Seward, 1990; Stefánsson et al., 2001, 2005; Nordstrom et al., 2005; McCleskey et al., 2014). According to the results of thermodynamic calculations Fe(II) in the form of the Fe^{2+} ion predominates in acid geothermal waters, whereas with increasing pH hydrolysis reactions stabilise Fe(III) relative to Fe(II) with $Fe(OH)_3^0$ and $Fe(OH)_4^-$ being the most important aqueous species (Heinrich and Seward, 1990; Stefánsson et al., 2001). Thermodynamic calculations, however, rely on overall redox equilibria that may not prevail in natural geothermal fluids (e.g. Stefánsson et al., 2005). Redox equilibrium is often attained at temperatures > 200 °C in the laboratory, yet the equilibrium state at depth in a natural system is rarely known. Previous studies suggest that partial equilibrium between the Fe(II)/$Fe(OH)_3$(s) may be closely approached in cold natural waters and circum-neutral to alkaline geothermal water in Iceland (Stefánsson et al., 2005) yet this remains to be further demonstrated through the compositional variation encountered in geothermal waters.

Active geothermal systems are characterized by steep gradients in temperature, pH and redox conditions. At depth, fluids may reach temperatures above 300 °C and are typically reduced, containing H_2 and H_2S (Stefánsson and Arnórsson, 2002), but tend to oxidize in the surface zone. Boiling, mixing, oxidation, and mineral precipitation and dissolution processes result in the formation of various surface geothermal features including warm and hot springs and pools that characterise the surface environment of active geothermal systems and vary significantly in water temperature, pH, and chemical compositions (Stefánsson et al., 2016; Björke et al., 2015). The dynamic chemistry and conditions in the surface geothermal environment support rich thermophilic microbial life that is capable of metabolizing the inorganic chemical energy available from various reactions involving the redox-active chemical components such as sulfur, iron, oxygen, hydrogen and nitrogen (e.g. Shock et al., 2010, and references therein). In the surface environment, redox disequilibrium is driven by the dynamic processes taking place at a relatively shallow depth in the systems (e.g. boiling, steam segregation, mixing) and the redox differences between the geothermal fluids and atmosphere (Stefánsson et al., 2005; Shock et al., 2010; Kaasalainen and Stefánsson, 2011). Therefore, there may not be redox equilibrium between Fe(II) and Fe(III), but the distribution of Fe (II) and Fe(III) may be dominated by the dissolution and precipitation kinetics, oxidation reactions, and/or the source(s).

With the aim to study the geochemistry and speciation of Fe(II), Fe (III), and Fe_{total} over the full range of temperature and pH conditions encountered in the surface geothermal environment in Iceland, samples of geothermal surface and well water were collected and analyzed for the Fe(II), Fe(III), and Fe_{total} concentrations in the < 0.2 μm filtered and acidified fraction. A field-deployed ion chromatography spectrophotometry (IC-Vis) method was used allowing the Fe(II) and Fe(III) determination to be carried out within minutes to a few hours of sampling in order to prevent and minimize post-sampling changes (Kaasalainen et al., 2016). Due to the complex nature of dissolved and solid Fe species that may be present and vary significantly across the conditions encountered in geothermal water, the importance of different size fractions was operationally defined by ultrafiltration and in-situ dialysis followed by determination of Fe_{total} and/or Fe(II) and Fe (III) in the filtrates and dialysates as appropriate. The results allow us to evaluate the major processes influencing Fe(II) and Fe(III) chemistry and speciation for a wide range of composition encountered in geothermal waters.

2. Ölkelduháls, Krýsuvík and Geysir geothermal areas

Samples of natural geothermal water were collected from high-temperature geothermal areas at Krýsuvík, Ölkelduháls, and Geysir located within or marginal to the active volcanic zone in south and southwest Iceland (Fig. 1). The chemical composition, pH, temperature, and redox state of the geothermal waters in these areas vary over a wide range (Arnórsson, 1985; Markússon and Stefánsson, 2011; Kaasalainen and Stefánsson, 2012). The compositional variation is a result of fluid evolution during which the reservoir fluid at depth, having circum-neutral pH and NaCl-type composition with Na, Cl, S, CO_2 and Si being the dominant dissolved elements, undergoes various processes including boiling, steam segregation, and/or mixing of various end-members and non-thermal ground or surface water, and water-rock interaction (Arnórsson, 1985; Arnórsson and Andrésdóttir, 1995; Markússon and Stefánsson, 2011; Kaasalainen and Stefánsson, 2012; Björke et al., 2015; Stefánsson et al., 2016).

Geothermal activity at the Krýsuvík and Ölkelduháls areas is characteristic of that associated with volcanic geothermal systems including mud pots, hot springs, warm streams, steam vents, steaming ground, and intense alteration of the associated rocks (Fig. 2A and B) (Arnórsson et al., 2007). Krýsuvík geothermal area, situated in the Reykjanes peninsula, has been extensively studied in the past with respect to alteration mineralogy and fluid chemistry (Arnórsson, 1969, 1987; Markússon and Stefánsson, 2011; Kaasalainen and Stefánsson, 2011, 2012 ; Ármannsson, 2016 and references therein). Maximum subsurface temperatures have been estimated at 260 °C (Arnórsson et al., 1975; Ármannsson, 2016). The present study focused on a small, easily accessible site known as Seltún, situated in the active geothermal area associated with the Sveifluháls hyaloclastite ridge formed during the last glaciation (Jónsson, 1978; Ármannsson, 2016) (Fig. 1). Ölkelduháls geothermal area belongs to the Hengill volcanic system, which is situated at the triple junction of the North American plate, the Eurasian plate, and the Hreppar microplate (Fig. 1). The rocks are made of basaltic hyaloclastite formations and lava flows. Subsurface temperatures ranging from 200 to 280 °C have been encountered upon drilling in the Ölkelduháls area (Steingrímsson et al., 1997; Ármannsson, 2016). In both areas, water temperatures at the surface range from ambient to boiling ~100 °C and pH typically lies in the range of 2–7. The water composition is dominated by S, Si, Ca, Mg, Al, Fe, typically with abundant reduced sulfur species, and in the case of circum-neutral pH, also CO_2 (Markússon and Stefánsson, 2011; Kaasalainen and Stefánsson, 2011, 2012). This is characteristic for steam-heated water forming upon vapor condensation into non-thermal water and subsequent oxidation, resulting in elevated SO_4 and metal concentrations but low Cl concentrations (Kaasalainen and Stefánsson, 2012; Stefánsson et al., 2016). In addition, springs rich in carbon dioxide are found at Ölkelduháls (Ármannsson, 2016).

The geothermal area at Geysir is a world-famous locality in the Southern Lowlands of Iceland, owing to its frequent geyser activity. The area is located marginal to the active volcanic belt (Fig. 1), and underlying basaltic rocks and rhyolite dome are younger than 800.000 years (Arnórsson, 1985; Ármannsson, 2016). The main geothermal activity is found within a small area characterized by numerous boiling hot springs, geysers, steam vents, and mud pots (Figs. 1 and 2D-G). Several warm and tepid springs occur outside the main field west of the Laugarfell rhyolite dome and a few kilometers north of the main active area along the Haukadalur valley (Fig. 1) and in addition, several hot-water wells have been drilled in the area (Figs. 1 and 2C). Water pH lies between ~2 and ~9, and the water types include steam-heated acid water, NaCl-type water, and mixtures with non-thermal surface and groundwater (Arnórsson, 1969, 1985). Maximum subsurface temperatures in the area have been estimated at 230–260 °C based on chemical geothermometry (Arnórsson, 1985; Kaasalainen and Stefánsson, 2012). Several studies have been carried out in the area with respect to fluid chemistry in general, as well as specific aspects such as sulfur speciation, silica sinter formation, and thermophilic microbial community (Arnórsson, 1985; Tobler et al., 2008; Tobler and Benning, 2011; Kaasalainen and Stefánsson, 2011).

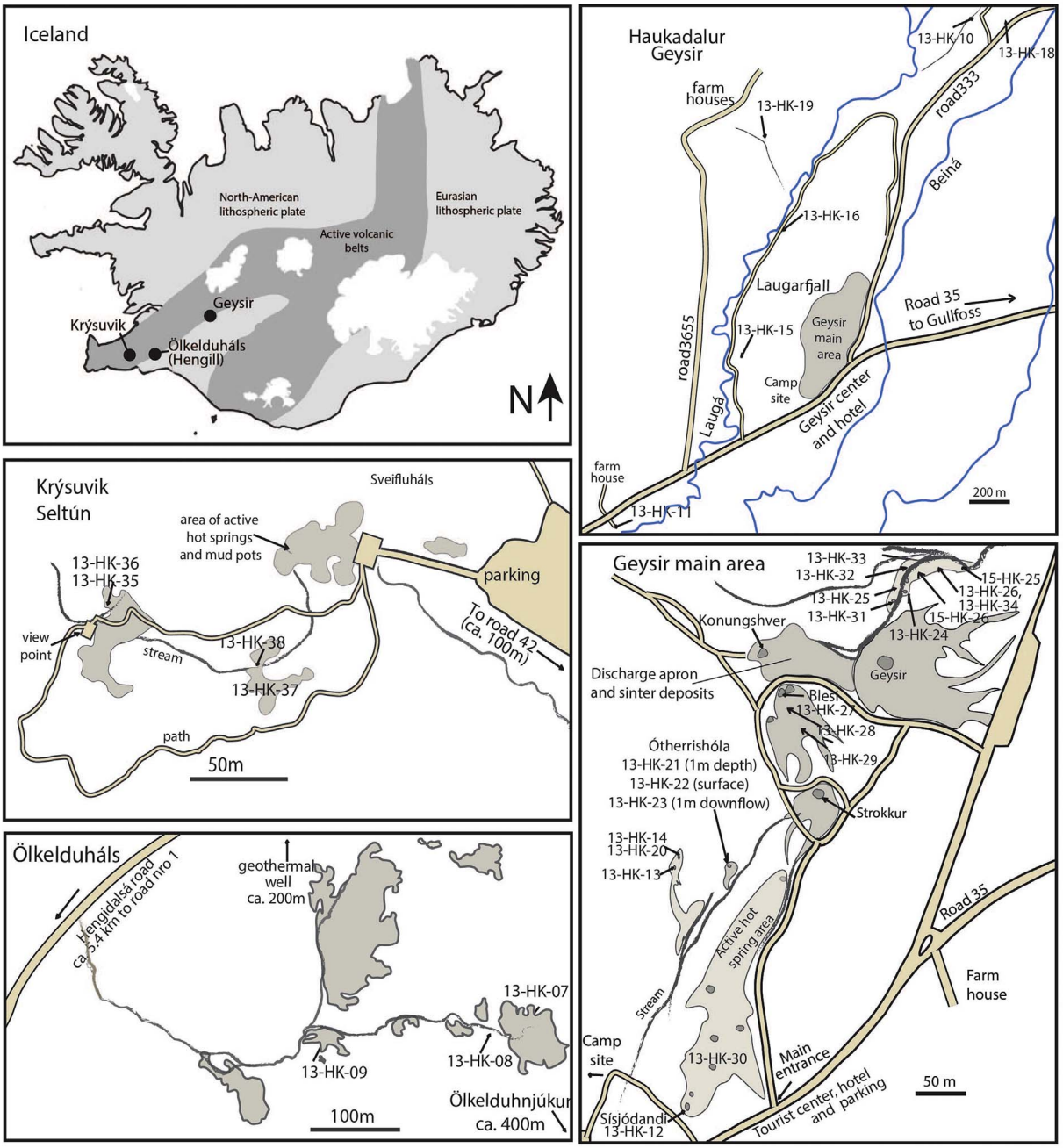

Fig. 1. Location of the active geothermal areas considered in this study, as well as the location of the sampling sites within each area.

3. Methods

3.1. Geothermal water sampling

A total of 35 geothermal water samples was collected from the Geysir, Krýsuvík and Ölkelduháls geothermal areas in 2013 and 2015. For the determination of dissolved Fe(II), Fe(III), and Fe_{total} concentrations, the water was filtered through < 0.2 μm cellulose acetate filter (Advantec) in-line by pumping the water through silicon tubing and a polypropylene filter holder. Samples for Fe(II) and Fe(III) determinations were collected into gas-tight glass bottles that were completely filled, immediately acidified (Merck Suprapur® HCl, 30%, 0.5 mL in 100 mL sample) and sealed, and stored in darkness until analysis. Additional samples for Fe_{total} determination were collected into PP bottles and acidified (Merck Suprapur® HCl, 0.5 mL in 100 mL sample). All tubing, filter holders, and sampling bottles used for the Fe (II) and Fe(III) sampling had been previously acid-washed and rinsed 2–3 times with deionized water, with additional 2–3 rinses with the filtered sample as appropriate. Samples were also collected for the determination of pH, CO_2, H_2S, and major cations and anions, and analyzed using a glass electrode, titrations, spectrophotometry, inductively coupled plasma atomic emission spectrometry (ICP-OES), and ion chromatography (IC) with the methods that have been previously described in detail (Eaton et al., 2005; Arnórsson et al., 2006; Stefánsson et al., 2007). Major and minor cations, including Fe, were determined in samples previously filtered through 0.2 μm filters and acidified (1 mL of 65% HNO_3 Suprapur® Merck, to 100 mL of sample) using inductively coupled plasma optical emission spectrometry (ICP-OES, Spectro Ciros Vision). Prior to ICP-OES analyses, the samples were typically diluted 2–10 times with dilute HNO_3 (1 mL of 65% HNO_3 Suprapur®, Merck, to 100 mL of MQ-water). The standards used for the ICP-OES analysis were in-house reference standards (SEL-11 and GYG-13) calibrated

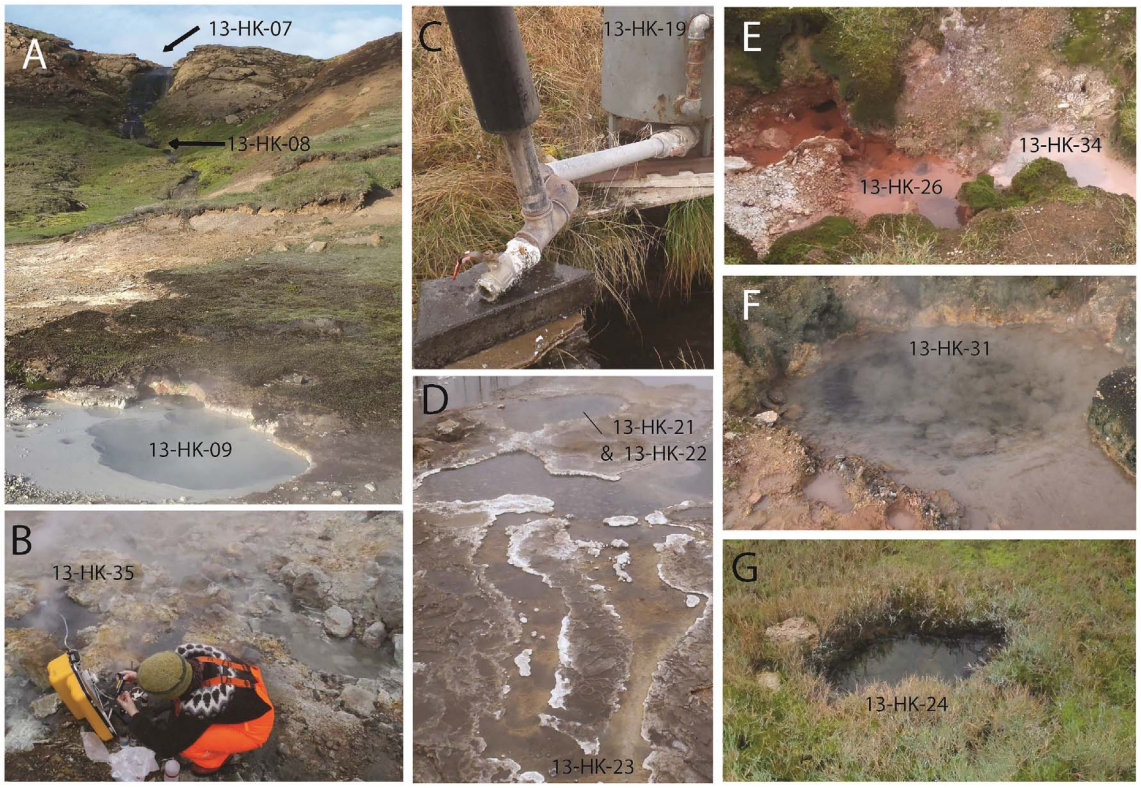

Fig. 2. Photos of selected sampling sites. **A.** An overview of the sampling sites at Ölkelduháls. **B.** Steam-heated water at Krýsuvík. **C.** Sub-boiling well in the greater Geysir area. **D.** Boiling hot spring at Geysir. **E.** Steam-heated acid water at Geysir. **F, G.** Mixed geothermal water at Geysir.

against commercial standards (SPEX CertiPrep). Anions (Cl^-, F^-, SO_4^{2-}, and in some cases $S_2O_3^{2-}$) were determined in filtered, unacidified samples using ion chromatography (Dionex, IC2000).

At the selected sites, the importance of Fe associated with the colloidal/nanoparticulate size fraction was studied. For this purpose, samples were filtered through 0.45 µm in-line filters, in addition to the 0.2 µm pore size filters. Moreover, dialysis tubes (Spectra/POR® 7, SpectrumLab®, 10 kDa and 1 kDa pore sizes) or pre-assembled floating dialysis devices (Float-a-Lyzer, SpectrumLab®, 8–10 kDa pore size) were deployed in-situ in selected springs and pools. The dialysis samplers had previously been filled, washed and equilibrated with deionized water changed several times, and were then deployed in-situ in the natural water for 1–2 days. Upon recovery, the liquid contained in the bags was sampled and acidified (0.5 mL conc. HCl in 100 mL sample, TraceSelect Ultra, Fluka), with subsequent determination of Fe(II) and Fe(III) concentrations as described in section 3.2.

The quality control and assurance included regular calibration, repeated analysis of blank solutions, and synthetic solutions of known concentrations within each batch, duplicate analysis and comparison of various analytical methods. Moreover, the charge balance of the samples was calculated at room temperature using the PHREEQC-program (Parkhurst and Appelo, 1999) with the phreeqc. dat thermodynamic database, and only samples with a charge balance within ±10% are considered, with the average charge balance error being +1.5% (ranging from −9.2 to 8.9%).

3.2. Fe(II) and Fe(III) analysis

The determination of Fe(II) and Fe(III) concentrations was carried out on-site in a field laboratory within 1–4 h of sampling using a Dionex ICS3000 ion chromatography (IC) system connected to a post-column reaction coil and a UV/Vis absorbance detector (AD25, Dionex, Thermo Scientific). The determination of Fe(II) and Fe(III) in geothermal water using the field-deployed IC-Vis method has been described and discussed in detail by Kaasalainen et al. (2016), along with a detailed account of the challenges associated with the Fe(II) and Fe(III) determination in the geothermal water. The IC-Vis method is based on the IC separation of Fe(II) and Fe(III) complexes with pyridine-2,6-dicarboxylic acid (PDCA) chelating agent contained in the eluent, followed by detection using post-column derivatization with 4-(2-pyridylazo)resorcinol (PAR) with absorbance detection at 530 nm. Sample injection into the injection valve system was either carried out manually using 3 mL pre-washed PP syringes or the Dionex AS autosampler unit, with a typical injection volume of 200 µL. The workable detection limits are 2–3 µg/L Fe(III) and 6–8 µg/L Fe(II). Calibrations were performed using standard Fe(III) solutions prepared gravimetrically from 1000 mg/L Fe(III)Cl_3 commercial standard (Merck) added to a 0.1 M HCl solution prepared by dilution of concentrated HCl (Merck, Suprapur®) in deionized water. Standard Fe(II) solutions were prepared by the reduction of Fe(III) standard solutions using ascorbic acid (50 µL per 10 mL solution) or by dissolving Mohr salt ($(NH_4)_2Fe(SO_4)_2{\cdot}6H_2O$, Fluka, puriss) in boiled and degassed (Ar) deionized water acidified to give 0.1 M HCl using concentrated HCl (Merck Suprapur®). For Fe_{total} determination the samples were treated with H_2O_2 (Suprapur®, Merck, 0.050 mL per 10 mL sample) in order to oxidize Fe(II) to Fe(III), followed by Fe_{total} analysis as Fe(III). If necessary, the samples were diluted gravimetrically 2–10 times with dilute 0.1 M HCl (Suprapur®, Merck) prior to Fe_{total} determinations. Additionally, Fe_{total} was determined using the ICP-OES along with major and minor cations as described in section 3.1, using samples that had been filtered through 0.2 µm filters and acidified (1 mL of 65% HNO_3 Suprapur® Merck, to 100 mL of sample) and in most cases diluted 2–10 time prior to analysis.

3.3. Geochemical calculations

The PHREEQC-program with the WATEQ4f.dat database (Ball and Nordstrom, 1991; Parkhurst and Appelo, 1999) was used for

Table 1
Concentrations of Fe(II), Fe(III) and selected major elements [μmol/L] in geothermal waters, Iceland.

Sample	Type[a]	T [°C]	pH	°C[b]	SiO_2	Cl	CO_2	H_2S	SO_4	Fe(II)[c]	Fe(III)[c]	Fe^c_{SUM}	$Fe_{total,\ IC}$[f]	$Fe_{total,\ ICP}$[g]
Sub-boiling wells in surroundings of the Geysir area														
13-HK-10	mgw	83	8.30	21	5203	2478	3689	6.6	703	< 0.15	0.05	< 0.2	0.11	< 0.8
13-HK-11	mgw	68	7.49	21	3360	1252	9153	na[d]	328	< 0.15	0.55	< 0.7	0.89	0.83
13-HK-19	mgw	51	7.81	23	1878	999	5152	na[d]	227	< 0.15	0.04	< 0.19	0.08	< 0.8
Spring and pools in the Geysir area and its surroundings														
13-HK-12	baw	99	9.50	21	5750	3329	2367	69.7	958	< 0.15	0.07	< 0.22	0.17	< 0.8
13-HK-21	baw	99	8.84	23	6275	3193	3126	83.2	923	< 0.15	0.06	< 0.21	0.11	0.62
13-HK-22	baw	99	8.85	23	6152	3162	3104	86.0	923	< 0.15	0.04	< 0.19	0.15	< 0.8
13-HK-23	baw	80	9.03	23	6247	3261	3032	32.0	964	< 0.15	0.04	< 0.19	0.11	< 0.8
13-HK-27	baw	95	9.75	23	8208	3522	1897	84.5	1018	< 0.15	0.11	< 0.26	0.06	< 0.8
13-HK-28	baw	82	9.76	23	8254	3620	1951	53.6	1023	< 0.15	< 0.035	< 0.19	0.05	< 0.8
13-HK-29	baw	65	9.77	23	8397	3645	1853	25.2	1048	< 0.15	< 0.035	< 0.19	0.04	< 0.8
13-HK-31	mgw	93	7.53	23	4461	2964	1507	2.5	1197	< 0.15	1.36	< 1.5	2.01	1.42
13-HK-30	mgw	78	6.38	23	4544	2349	832	na[d]	2264	< 0.15	0.15	< 0.30	0.16	< 0.8
13-HK-15	mgw	37	7.45	21	1473	848	2689	na[d]	168	< 0.15	2.08	< 2.3	2.36	4.4
13-HK-16	mgw	41	8.30	21	1574	700	1949	na[d]	151	< 0.15	< 0.035	< 0.19	0.17	< 0.8
13-HK-17	mgw	36	7.54	23	1526	788	1680	na[d]	173	< 0.15	4.90	< 5.1	7.49	8.71
13-HK-18	mgw	38	7.56	23	1601	687	1869	na[d]	199	< 0.15	0.62	< 0.77	0.66	0.65
13-HK-13	mgw	42	6.73	21	1322	588	2083	na[d]	188	< 0.15	0.05	< 0.20	0.16	< 0.8
15-HK-29	mgw	38	6.26	23	2859	3039	3361	1.7	1256	2.6	8.84	11.5	na	5.10
13-HK- 20	mgw	27	6.27	23	1162	385	2382	na[d]	211	< 0.15	0.42	< 0.57	1.02	1.09
13-HK-14	mgw	30	5.92	20	1149	377	3624	na[d]	221	< 0.15	0.40	< 0.55	1.24	0.93
13-HK-24	mgw	48	5.85	23	1923	152	1154	2.1	445	3.6	2.98	6.58	8.99	10.7
13-HK-32	shaw	73	3.60	23	2210	420	na	< 1	1265	5.7	1.61	7.34	6.64	8.60
15-HK-26	shaw	45	2.87	23	3327	388	na	< 1.5	1584	4.9	14.2	19.1	na	18.8
13-HK-25	shaw	59	2.92	23	3411	151	294	0.5	1830	32.3	8.17	40.5	39.7	44.6
13-HK-26	shaw	75	2.74	23	3215	84	169	< 1	1399	7.3	1.20	8.49	7.89	8.17
13-HK-34	shaw	71	2.66	23	3260	89	1529	3.0	1727	8.3	3.81	12.1	10.8	15.4
13-HK-33	shaw	62	2.49	23	3515	71	793	< 1	3626	11.9	41.7	53.7	53.6	53.6
15-HK-25	shaw	40	2.46	23	3635	100	na	< 1.5	3643	45.8	99.5	145	na	148
Springs and pools in Krýsuvik area														
13-HK-37	shaw	38	3.41	22	1092	404	na	67.7	2346	136[e]	5.71		141	135
13-HK-38	shaw	60	3.66	22	1157	374	na	2.6	495	21.8	2.73	24.6	23.0	26.2
13-HK-35	shnw	88	6.35	22	1347	364	299	82.5	1612	0.8	0.61	1.4	0.87	< 0.8
13-HK-36	shnw	32	6.17	22	487	414	936	456	481	0.7	0.75	1.5	1.68	2.33
Springs and pools in Ölkelduháls area														
13-HK-09	shaw	70	3.13	23	2199	129	808	< 1	865	31.2	2.30	33.5	33.7	36.7
13-HK-07	shnw	82	6.37	23	2470	117	2427	19.9	925	< 0.15	< 0.1	< 0.25	0.59	< 1
13-HK-08	shnw	43	6.7	23	2461	125	2640	2.1	786	1.9	0.88	2.7	4.15	2.1

[a] Water type: boiled alkaline water (baw), mixed geothermal water (mgw), steam-heated neutral water (shnw), steam-heated acid water (shaw).
[b] Temperature of the pH measurement.
[c] Determined in the 0.2 μm filtered and HCl-acidified (0.1 M fraction) using the UV-Vis method in field within 1–4 h of sampling.
[d] No H_2S present based on previous studies (data file of the Geysir research group, University of Iceland).
[e] Value calculated based on the measured Fe(III) and $Fe_{total,\ IC}$.
[f] Fe_{total} concentrations in 0.2 μm filtered fraction determined using the IC-Vis method in H_2O_2 treated samples.
[g] Fe_{total} concentrations in 0.2 μm filtered fraction determined using ICP-OES.

geochemical calculations including aqueous species distribution and mineral saturation state calculations. The calculations were conducted at 25 °C and 1 bar. The reason for this is that the samples were cooled down to room temperature prior to analysis, and therefore may not represent the actual geothermal water temperature. Mineral solubility constants for amorphous Fe(III) hydroxide, goethite, mackinawite, and pyrite were those in the wateq4f database, whereas the solubility of 2 and 6-line ferrihydrite were those compiled and reported by Stefánsson (2007). These constants and the thermodynamic data in the WATEQ4f-database were further used in the calculation of the equilibrium constants for various redox reactions involving the aqueous Fe(II) and Fe (III) species and the relevant Fe solid phases, as well as the construction of the pe-pH diagram.

4. Results and discussion

4.1. Water composition

The waters had temperatures in the range of 27–99 °C, pH between 2.46 and 9.77, and total dissolved solids (TDS) ranging from 155 to 1090 mg/L. The chemical composition of the water sampled is given in Table 1. Based on the major element composition, pH, and temperature, the geothermal surface water samples are divided into boiled alkaline water, steam-heated acid water, steam-heated neutral water, and mixed geothermal water (Table 1, Fig. 3). Boiled alkaline water samples discharged by boiling hot springs had pH > 8.5 and NaCl-type composition with elevated Na, Si, Cl, and ΣCO_2 concentrations, and very low Mg concentrations. Steam-heated acid water samples, typical for mud pots and some streams, had acid pH < 4, elevated concentrations of SO_4, and many metals, but low Cl concentrations. Steam-heated neutral water had pH of ~6–8, low Cl concentrations, and often high ΣCO_2 concentrations compared to steam-heated acid water. Mixing between the above waters as well as non-thermal water results in the formation of mixed waters (Kaasalainen and Stefánsson, 2012; Björke et al., 2015; Stefánsson et al., 2016). The mixed water considered in this study, referred to as mixed geothermal water, predominantly represents mixtures between the geothermal reservoir water and non-thermal water in the Geysir area and its surroundings (Table 1, Arnórsson, 1985). Boiled alkaline water, mixed geothermal water and steam-heated neutral water are observed in the Geysir area, whereas steam-heated neutral and acid water predominate at Krýsuvík and Ölkelduháls. Water sampled from the hot-water wells in the proximity of the Geysir area discharge the unboiled aquifer water that has undergone variable extent of mixing with non-thermal water (Arnórsson, 1985; Arnórsson and

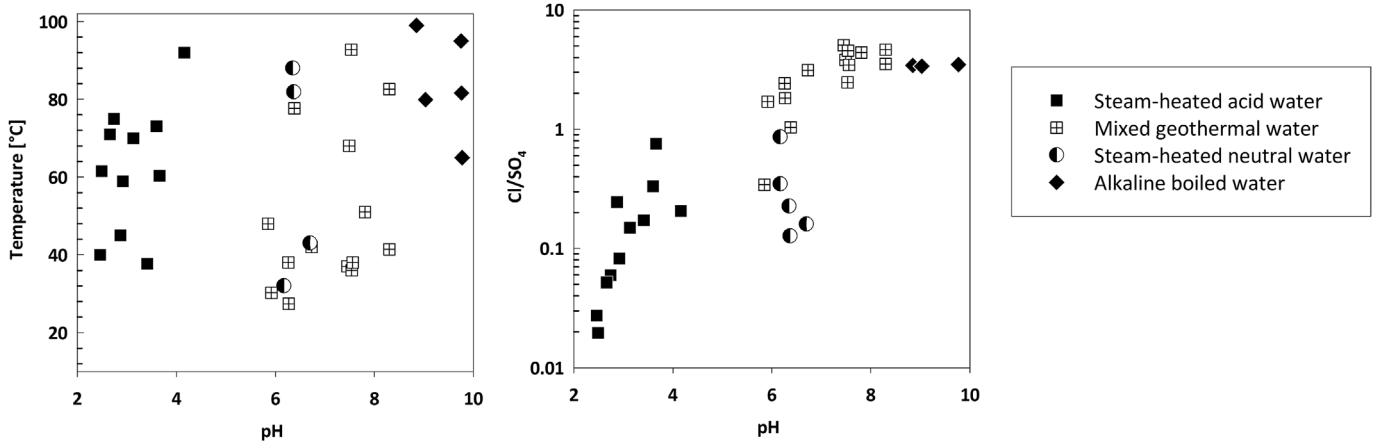

Fig. 3. The relationship between the water temperature, pH and Cl/SO_4 in the studied geothermal waters.

Andrésdóttir, 1995). The composition of the sub-boiling well waters is of the NaCl type similar to that of alkaline boiled water, yet the two differ in pH and absolute concentrations (Table 1) as boiling has resulted in loss of ΣCO_2, an alkaline pH, and elevated non-volatile concentrations in alkaline boiled water, and mixing with non-thermal water have resulted in higher Mg but dilution of non-volatiles in sub-boiling well water.

4.2. Fe_{total}, Fe(II), and Fe(III) concentrations

A systematic relationship can be observed between the Fe_{total}, Fe(II) and Fe(III) concentrations and the water pH. Dissolved iron concentrations (< 0.2 μm fraction) in the geothermal waters in Iceland range from < 0.01 μmoL/L to > 5 mmoL/L as reported by Kaasalainen and Stefánsson (2012) (Fig. 4). The Fe(II) and Fe(III) concentrations of water sampled in this study were in the ranges < 0.15–136 μmoL/L and < 0.1–100 μmoL/L, respectively (Figs. 4 and 5). Geothermal waters having alkaline pH are characterized by low Fe_{total} concentrations, with Fe(III) being the dominant oxidation state and Fe(II) concentrations below detection. With decreasing pH, the Fe_{total} concentrations increase with Fe(II) becoming increasingly more important relative to Fe(III) in steam-heated waters, accounting for 22–97% and 50–97% of Fe_{total} in steam-heated acid and neutral waters, respectively. Restricted trends may be observed between the water temperature and Fe_{total} concentrations, except for the steam-heated acid waters in which Fe_{total} concentrations show an increasing trend with decreasing temperature.

As discussed in detail by Kaasalainen et al. (2016), some differences are observed between the sum of the Fe(II) and Fe(III) determined by the IC-Vis method in the field and the total Fe concentrations determined by the ICP-OES or IC-Vis methods later in the laboratory (Table 1). However, in many cases, the comparison is difficult due to low concentrations. These differences are considered to arise from the general challenges in sampling and analysis of concentrations close to the instrumental detection limits, as well as the range of Fe forms that may have been present in the samples including filter passing colloidal/nanosized Fe solids (Fe(III) (oxy)hydroxides, Fe(II)-sulphides, organic colloids), or strong organic complexes. These different Fe forms may not be accounted for in the same way for each method either due to the nature of the analysis or due to varied sample storage length prior to analysis. Kaasalainen et al. (2016) showed that the sum of the Fe(II) and Fe(III) concentrations and the Fe_{total} determined at the same time point using the IC-Vis method in the laboratory were in excellent agreement but the Fe_{total} concentrations determined using the IC-Vis method, which only picks up weakly complexed and hydrated Fe species, were typically somewhat lower than those obtained by the ICP-OES method. This suggests that some Fe forms were present that were not detectable by the IC-Vis method even after treatment with hydrogen peroxide but were broken down in the plasma and therefore included in the Fe concentrations determined using the ICP-OES method.

4.3. Processes affecting Fe_{total}, Fe(II) and Fe(III) concentrations in geothermal water

The major processes that are considered to influence the concentrations and speciation of Fe in geothermal water include water-rock interaction, boiling and mixing, and redox reactions (e.g. Stefánsson et al., 2001, 2005; Kaasalainen and Stefánsson, 2012; Hardardóttir et al., 2009; Kaasalainen et al., 2015). In addition, microbiological reactions may also play a role, in particular in the acid pH conditions, in which the kinetics of chemical Fe(II) oxidation are significantly slower than at a higher pH (Stumm and Morgan, 1981; Kappler and Straub, 2005).

In the basaltic environment in Iceland, boron is considered to be mobile upon water-rock interaction and has been used as an indicator of rock leaching (Arnórsson and Andrésdóttir, 1995). In agreement with the findings of Kaasalainen and Stefánsson (2012), the Fe to B ratios in water samples considered in this study are lower than the corresponding basaltic rock ratio indicating Fe to be immobile and possibly taken up by secondary minerals.

Several Fe-containing alteration mineral phases have been observed in the surface geothermal environment in Iceland including sulfides (predominantly pyrite, marcasite) and various (hydr)oxides including amorphous Fe(III) hydroxide, goethite, and hematite (Arnórsson, 1969; Markússon and Stefánsson, 2011; Björke et al., 2015). The distribution of Fe minerals is related to the intensity of the surface hydrothermal activity, oxidation front, and the water type (Markússon and Stefánsson, 2011; Björke et al., 2015). In addition to these minerals, magnetite and pyrrhotite have been identified in the subsurface alteration products in the drill cuttings and well scales from active geothermal systems (Steinthórsson and Sveinbjörnsdóttir, 1981; Hardardóttir et al., 2009). Moreover, Fe-silicate has been observed forming from boiled high-temperature reservoir fluids and in the surface geothermal environment (Konhauser and Ferris, 1996; Tobler et al., 2008; Hardardóttir et al., 2009 and references therein). To our best knowledge, Fe-sulfate or hydroxy sulfate minerals, such as jarosite, melanterite or schwertmannite, have not been reported to occur in the geothermal surface environment in Iceland.

In Fig. 5, the Fe(II) and Fe(III) concentrations in geothermal water are shown together with the mineral solubilities of selected Fe minerals observed in the surface geothermal environment in Iceland including ferrihydrite, goethite, schwertmannite, mackinawite, and pyrite. The saturation state with respect to Fe(II) containing minerals cannot be evaluated for boiled alkaline water and mixed geothermal water as Fe (II) concentrations are below the detection limit. For steam-heated

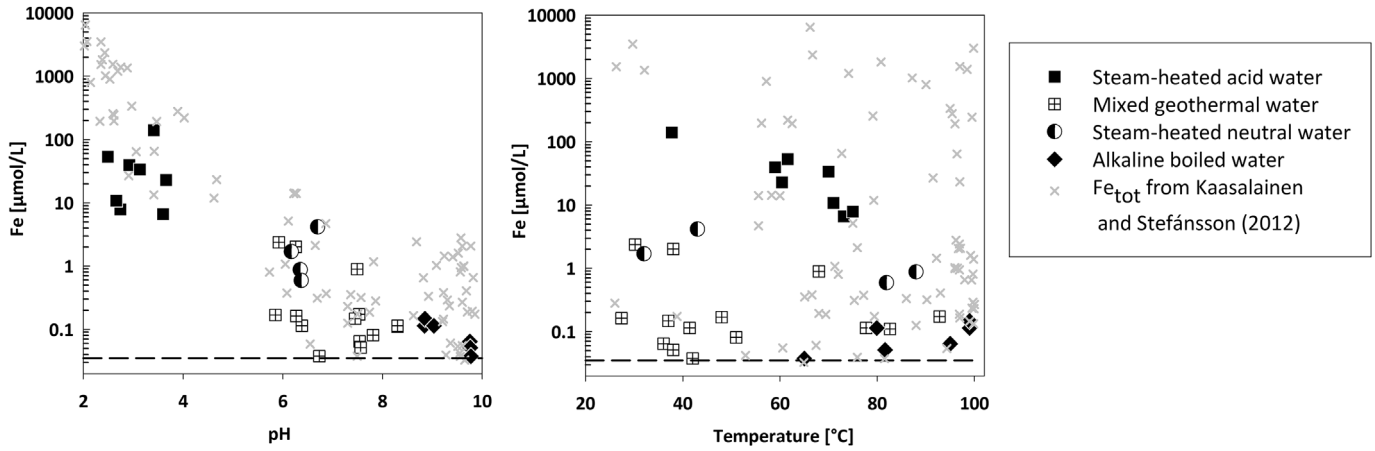

Fig. 4. The relationship between the water pH and temperature and Fe concentrations in geothermal waters in Iceland. For this study, Fe concentrations shown are the sum of Fe(II) and Fe(III) concentrations in < 0.2 µm filtered and acidified fraction. Also shown are the Fe_{total} concentrations in surface geothermal waters in Iceland as reported by Kaasalainen and Stefánsson (2012).

neutral water, the Fe(II) concentrations agree well with the solubility of mackinawite at relevant sulfide concentrations i.e. those observed in the Krýsuvík and Ölkelduháls geothermal areas. This is good agreement with the dark gray color of such water (Fig. 2) and the black precipitates observed during filtration. Mackinawite has not been reported from the surface alteration in Iceland, but nanocrystalline mackinawite and amorphous FeS are typically the initial Fe-sulfides precipitating in anoxic, sulfidic solutions or upon anoxic-oxic transition, followed by transformation to more stable phases such as pyrite (Schoonen and Barnes, 1991; Benning et al., 2000). The steam-heated acid waters are undersaturated with respect to mackinawite but supersaturated with respect to pyrite as commonly observed under such conditions. Pyrite supersaturation is commonly observed and pyrite is commonly found in the alteration product, yet it may not necessarily precipitate directly from solution. Alternatively, the oxidation of sulfide by oxidants such as molecular oxygen and ferric oxyhydroxide minerals may lead to the formation of elemental sulfur, and by further reaction with sulfide, polysulfide. Pyrite may form via the polysulfide pathway in at least some of these environments (Rickard and Luther, 1997; Butler et al., 2004). Thus, host rock leaching, redox reactions or microbiological reactions may control the Fe(II) concentration in the steam-heated acid water.

The Fe(III) concentrations in boiled alkaline water and many steam-heated acid waters appear to be close to saturation with respect to amorphous and 6-line ferrihydrite, respectively (Fig. 5). Such amorphous or poorly crystalline phases tend to be the first Fe(III) hydroxide phase to precipitate from solution, with the reported solubility constants varying over a large range due to the varying crystallinity and aging effects (Nordstrom et al., 1990; Majzlan et al., 2004). In addition to steam-heated acid water and boiled alkaline water, the Fe(III) concentrations of many neutral-pH samples are also found in close agreement with the amorphous Fe(III) hydroxide solubility; however, several samples show significant supersaturation with respect to this phase as discussed in the following section (4.4). These findings suggest that Fe (III) concentrations in many geothermal waters may be controlled by ferric hydroxide solubility, in agreement with previous studies (Stefánsson et al., 2005).

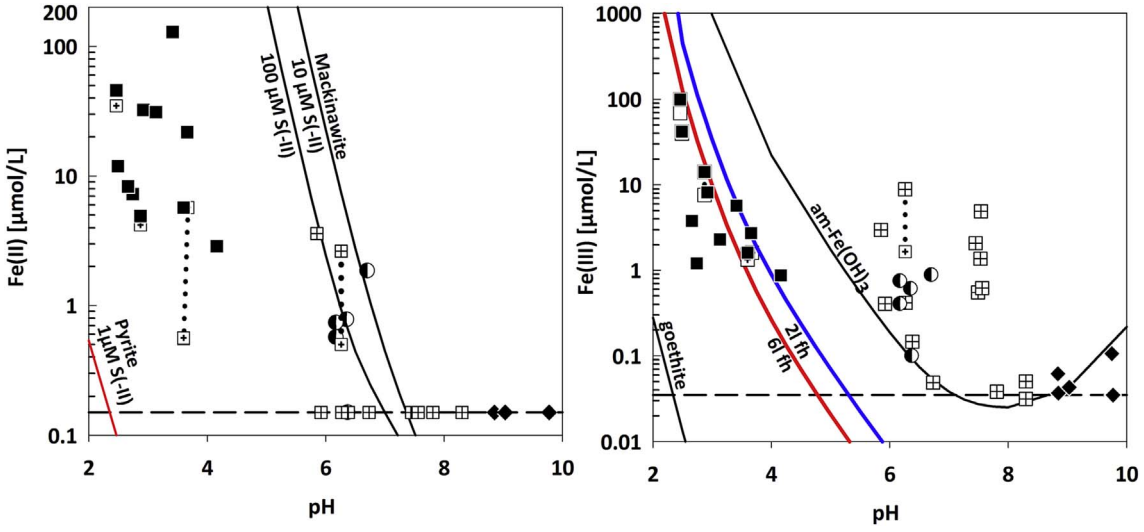

Fig. 5. The relationship between the water pH and the concentrations of Fe(II) and Fe(III) in < 0.2 µm and acidified fraction of geothermal water samples. Note that the symbols are as in Fig. 4. Where dotted lines connect two symbols at different concentrations, the Fe(II) and Fe(III) concentrations in the < 10 kDa fraction are also shown in addition to the < 0.2 µm fraction (see section 4.3). Shown are also the solubility lines for selected Fe(III) and Fe(II) minerals. The solubility constants for amorphous ferric hydroxide, goethite, pyrite, mackinawite are from the wateq4f database (Ball and Nordstrom, 1991), whereas those of 2- and 6-line ferrihydrite from Stefánsson (2007) The solubility of Fe(III) minerals was calculated in pure water; mackinawite in the presence of dissolved sulfide in the range of 1–100 µmoL/L, and pyrite in the presence of 1 µmol/L of sulfide and 2 mmoL/L SO_4 and pe assigned to the sulfide/sulfate redox pair.

4.4. Nanoparticulate Fe

A significant population of samples including both steam-heated neutral water and mixed geothermal water contained Fe(III) in higher concentrations as expected based on the solubility of amorphous Fe(III) hydroxide, the most soluble Fe(III) containing phase (Fig. 5). The reason for this finding is considered to be the presence of nanoparticulate Fe in the geothermal water, which passes through the 0.2 μm pore size filter during sampling, dissolves upon sample acidification, and is consequently interpreted as dissolved Fe. Nano-sized Fe solids have previously been reported in natural and experimental solutions by several authors and involve both Fe(II) and Fe(III) valence states (e.g. Fox, 1988; Benning et al., 2000; Pokrovsky and Schott, 2002; Cornell and Schwertmann, 2003).

In order to study the potential occurrence of nanoparticulate Fe samples in the geothermal waters under study, the different size fractions of Fe were operationally determined at selected locations. This was done by an ultrafiltration method or by analyzing the inner solutions from dialysis devices deployed in-situ in geothermal water, in addition to filtering the sample through 0.45 μm and 0.2 μm pore size filters. The nanoparticulate Fe may pass through the 0.45 and 0.2 μm filters, whereas the fraction passing through the < 10 kDa and in particular the < 1 kDa membrane pore size may be considered to represent a truly dissolved fraction (Fox, 1988; Batley, 1989). Therefore, the difference between the Fe concentrations determined in the < 0.2 μm filtered and < 1–10 kDa size fractions represents the nanoparticulate Fe fraction. Examples of the concentrations of Fe(II) and Fe(III) determined in the different size fractions are shown in Fig. 6 and listed in Table 2. Moreover, the Fe concentrations determined in the < 0.2 μm and the truly dissolved fraction are shown in Fig. 5 where two symbols are connected with dotted lines. In some cases, there is a good agreement between Fe(II) and Fe(III) concentration in the < 0.2 μm and < 10 kDa filtered fraction, but in several others these concentrations are considerably different, with much lower Fe(II) and Fe(III) concentration in the < 10 kDa filtered fraction compared with the < 0.2 μm filtered fraction. These findings suggest that in some cases, a significant fraction of Fe passing the standard filters may not be truly dissolved but rather present in a nanosized solid form. Upon acidification, these nanosized Fe solids may dissolve, resulting in an overestimation of the truly dissolved Fe(II) and/or Fe(III) concentration in thermal water. The discussion on their origin is outside the scope of this study, but the possible explanations may, for example, include mixing, cooling, and oxidation processes taking place along the flow path the geothermal fluid, or in some cases, the presence of Fe-rich organic colloids.

4.5. Fe(II)and Fe(III) aqueous speciation

Using the analyzed Fe(II) and Fe(III) concentrations in the geothermal waters, the thermodynamic speciation of each oxidation state was calculated independently from the redox potential (pe) value. The species distribution of Fe(II) and Fe(III) in the dissolved fraction calculated this way is shown in Fig. 7 for the various types of geothermal waters sampled in this study. From Fig. 7 it is evident that the distribution of aqueous Fe species is affected by the water type, which in turn reflects the pH and redox conditions as well as major ion composition of the water. In boiled alkaline water and sub-boiling aquifer water, only Fe(III) was detected and was present predominantly as hydrolyzed Fe(III) species. Also Fe(II) may have been present at low concentrations below the detection limit, and in such a case may be expected as Fe^{2+} or carbonate species. In mixed geothermal water, hydrolyzed Fe(III) species typically dominate, together with Fe^{2+} in cases where Fe(II) is present. In steam-heated neutral water, Fe^{2+} and Fe(II)-sulfide species are important, together with significant Fe(III) hydrolysis species. In both mixed geothermal water as well as steam-heated neutral water, minor Fe(II) sulfate and carbonate species are suggested. In steam-heated acid water, Fe^{2+} and Fe(III)-sulfate species

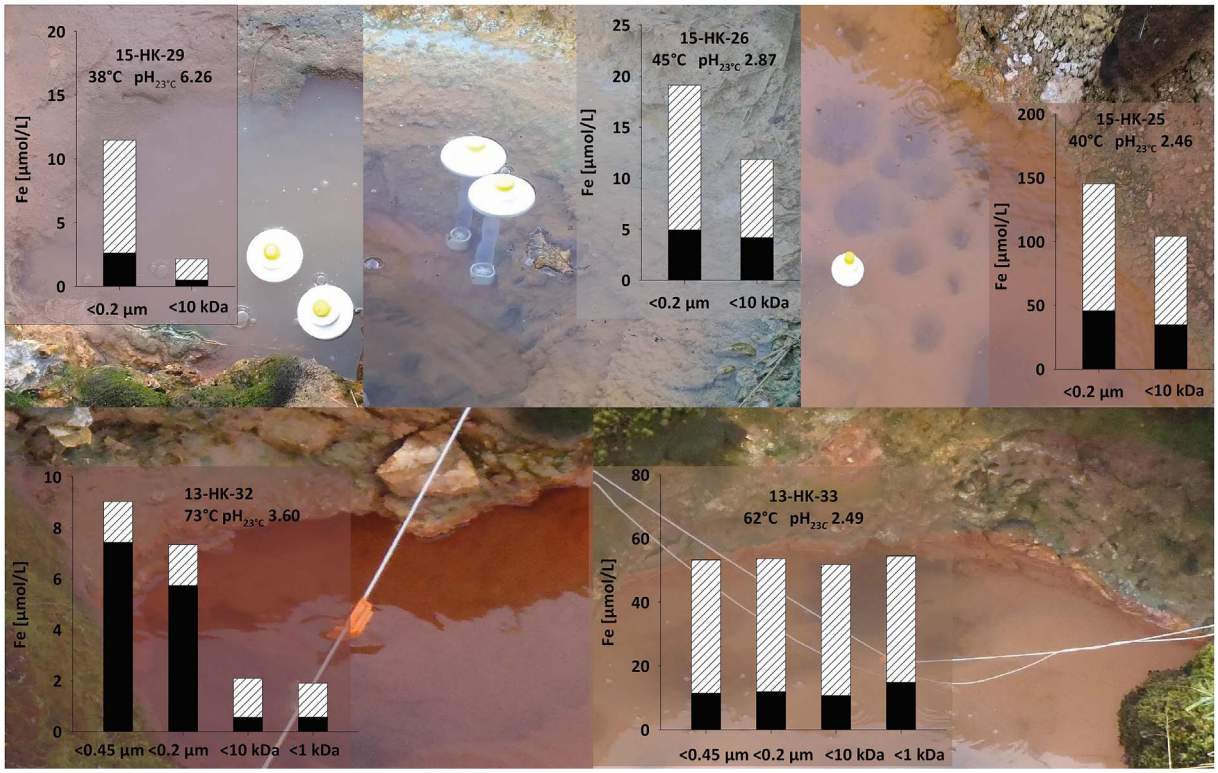

Fig. 6. Concentrations of Fe(II) (black bars) and Fe(III) (lined bars) in different size fractions sampled using in-line one-step filtration through 0.2 and 0.45 μm filters and in-situ dialysis to separate the < 1 kDa and < 10 kDa fractions. The concentrations measured in the < 10 kDa fractions are thought to represent the truly dissolved Fe(III) and Fe(III) concentrations, whereas the difference between such truly dissolved and < 0.2 and < 0.45 μm fraction is thought to represent the nanoparticulate Fe. The sampled waters had acid to neutral pH values and temperature between 38 and 73 °C.

Table 2
Examples of concentrations of Fe(II), Fe(III) and the sum of the two (Fe_{SUM}) (in μmol/L) in different size fractions collected using in-situ dialysis.

Sample #	Temp. [°C]	pH at 22C	Fe(II)	Fe(III)	Fe_{SUM}	Fe(II)	Fe(III)	Fe_{SUM}	Fe(II)	Fe(III)	Fe_{SUM}	Fe(II)	Fe(III)	Fe_{SUM}
			< 0.45 μm			< 0.2 μm			< 10 kDa			< 1 kDa		
13-HK-32	73	3.60	7.4	1.6	9.0	5.7	1.6	7.3	0.6	1.5	2.1	0.6	1.3	1.9
13-HK-33	62	2.49	11.5	41.8	53.3	11.9	41.7	53.7	10.7	41.2	51.8	14.9	39.6	54.5
15-HK-29	38	6.26	na	na	na	2.6	8.8	11.5	< 0.5	1.6	1.6	na	na	na
15-HK-26	45	2.87	na	na	na	4.9	14.2	19.1	4.2	7.6	11.8	na	na	na
15-HK-25	40	2.46	na	na	na	45.8	99.5	145.4	34.9	69.2	104.1	na	na	na

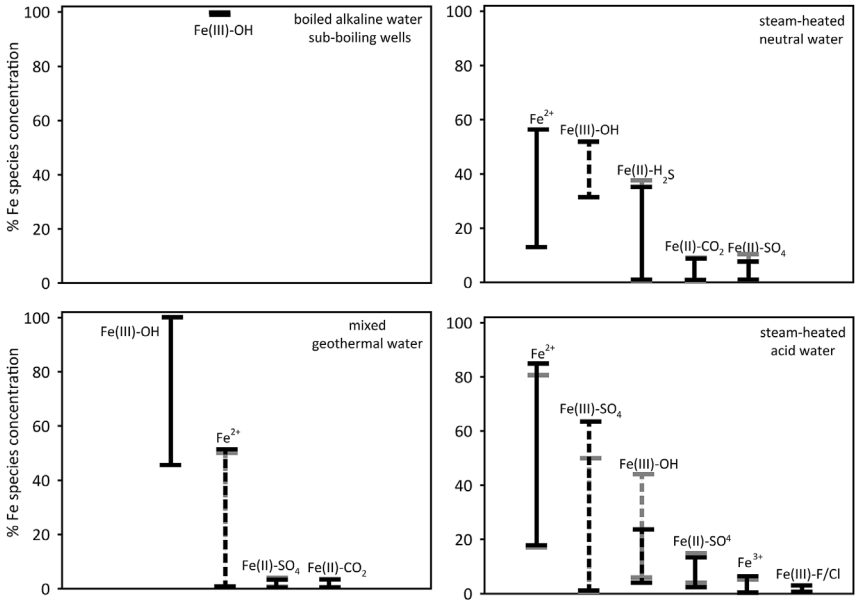

Fig. 7. Distribution of aqueous Fe(II) and Fe(III) species in different thermal water types, calculated based on the Fe(II) and Fe(III) concentrations determined in the respective waters. The species distribution calculated at 25 °C and discharge temperature is shown with black and gray colored symbols, respectively.

predominate, with Fe(III) hydrolysis species and minor Fe(III)-sulfate and free Fe^{3+} species present as well. Thus, it is clear that distribution of Fe species varies greatly over the different water types.

The Fe(II) and Fe(III) concentrations determined and the calculated aqueous species distribution can be used to calculate a pe-value based on the following equations:

$$Fe^{2+} = Fe^{3+} + e^- \quad (1)$$

$$pe = - \log [e^-] \quad (2)$$

$$pe = \log[Fe^{3+}] - \log[Fe^{2+}] - \log K \quad (3)$$

Where $[e^-]$, $[Fe^{3+}]$, and $[Fe^{2+}]$ stand for the activities of an electron (e^-), Fe^{3+} and Fe^{2+} ions in the solution, and K for the equilibrium constant for the reaction (1).

For samples having Fe(II) concentrations below detection limits, the value at the detection limit was used to give a maximum estimate of the Fe(II) concentrations that may have been present, and thus the respective pe value gives a minimum estimate of the pe value for the Fe^{2+}/Fe^{3+} pair. The relationship between the water pH and pe value calculated for the Fe^{2+} and Fe^{3+} ratio is shown in Fig. 8, and shows a systematic trend.

There are several other possible redox reactions among Fe minerals and aqueous species, including the following reactions involving the ferric hydroxide and mackinawite (FeS) solid phases:

$$Fe(OH)_3(s) + 3H^+ + e^- = Fe^{2+} + 3H_2O \quad (4)$$

$$Fe^{3+} + HS^- + e^- = FeS(s) + H^+ \quad (5)$$

and similarly to what has been described above, a value for redox potential pe can be calculated based on these reactions. Moreover, many other elements present in more than one oxidation state, such as hydrogen, oxygen, sulfur, nitrogen and carbon, may be involved in the redox reactions of Fe(II) and Fe(III). The exact reactions, however, are difficult to evaluate as in order to calculate the pe values for these reactions analytical data must be available for all the species involved. Reactions (4) and (5) involve ferric hydroxide (amorphous or 6-line ferrihydrite) and mackinawite, both of which were observed close to saturation in the studied waters (section 4.3), and may thus be of importance in the waters studied. For the waters sampled, the typically most important sulfur species sulfate (S(VI)) and sulfide (S(-II)) were determined, thus allowing us additionally to estimate the pe value for the following reaction:

$$SO_4^{2-} + 10\ H^+ + 8e^- = H_2S + 4H_2O \quad (6)$$

The pe values estimated for these three reactions are shown in Fig. 8 for comparison with those calculated for the Fe^{2+}/Fe^{3+} pair (reaction 1). In the case of redox equilibrium between the different pairs, these pe values should agree. Indeed, reasonable agreement is observed between the pe calculated for the Fe^{2+}/Fe^{3+}, mackinawite/Fe^{3+}, and $Fe^{2+}/Fe(OH)_3(s)$ pairs, assuming the maximum solubility product for ferrihydrite (logK = 4.891) reported for freshly precipitated amorphous ferric hydroxide by Ball and Nordstrom (1991), in boiled alkaline water, steam-heated neutral geothermal water, and in many mixed waters. The exceptions include samples 13-HK-17, 13-HK-31, 13-HK-15, and 13-HK-18, and the reason is thought to be the possible inclusion of filter passing colloidal Fe in the samples as discussed in section 2.3. Also for some steam-heated acid waters, a reasonable agreement is observed between the Fe^{2+}/Fe^{3+} and ferrihydrite assuming a minimum solubility constant similar to that of 6-line ferrihydrite and in a few cases between the Fe^{3+}/mackinawite and H_2S/SO_4 redox pairs. This, however, is not the case for all samples, suggesting that Fe redox disequilibrium may prevail for those waters.

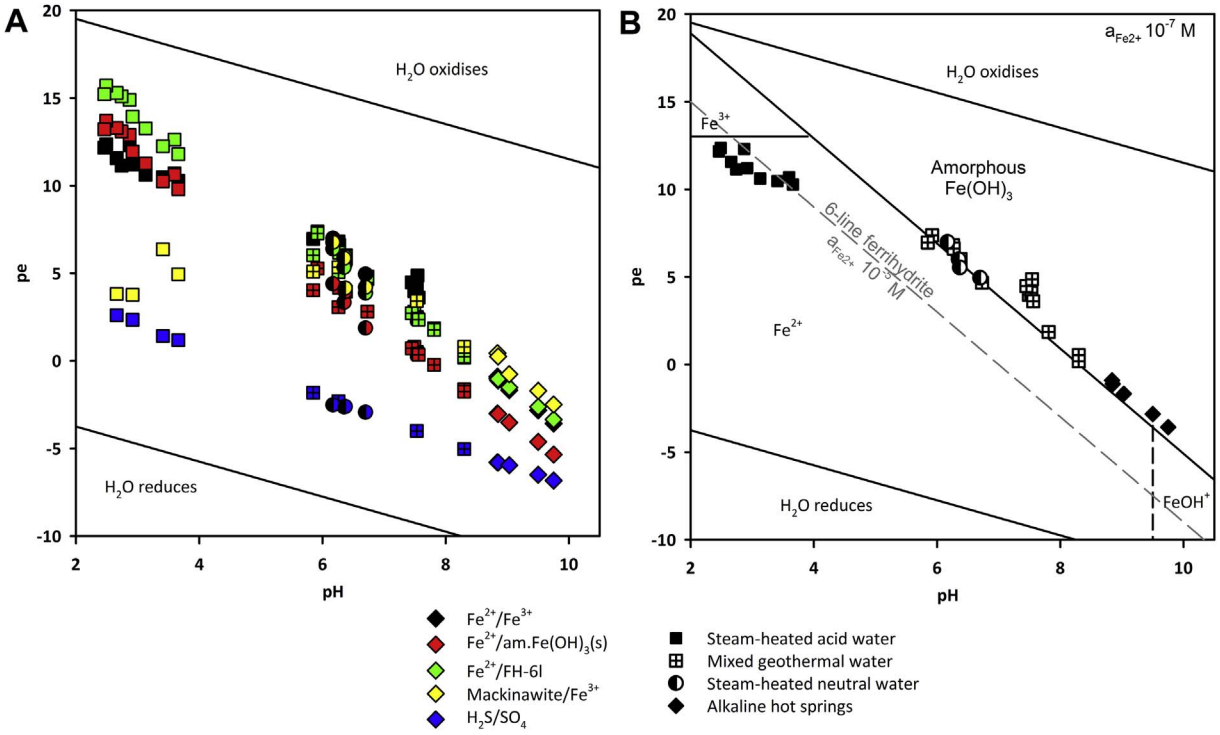

Fig. 8. A. The relationship between the water pH and pe-values calculated for selected redox pairs involving aqueous and solid Fe(II) and Fe(III) species. The different redox pairs, represented by different colors, include Fe^{2+}/Fe^{3+}, Fe^{2+}/amorphous Fe(III) hydroxide, Fe^{2+}/6-line-ferrihydrite, mackinawite/Fe^{3+}, and H_2S/SO_4 according to reactions (1) and (4)–(6) (section 4.5). Water types are represented by different symbol shapes. **B.** pe-pH diagram for the selected aqueous and solid Fe species. The symbols present pe-values for the Fe^{2+}/Fe^{3+} pair (reaction 1, section 4.5), based on the Fe^{2+} and Fe^{3+} activities calculated from the measured Fe(II) and Fe(III) concentrations in different water types. The stability fields for the solid phases were calculated assuming the activity of Fe^{2+} at 10^{-7} and 10^{-5} M in the case of amorphous Fe(III) hydroxide and 6-line ferrihydrite, respectively, and the ratio of 1 for the activity of aqueous Fe^{2+} and Fe^{3+}. In both A and B, the value of the detection limit was used for the samples with Fe(II) concentrations below the detection limit, thus representing the maximum Fe(II) present and the minimum estimation of the respective pe-value in the samples. (For interpretation of the references to colour in this figure legend, the reader is referred to the web version of this article.)

At pH ~6 and above, the fast kinetics of the Fe^{2+} oxidation resulting in the precipitation of Fe(III) hydroxide and possibly Fe(II) sulfide may result in a local equilibrium between the dissolved Fe(II), Fe(III) with the Fe-containing solid phases. Despite the local equilibrium that may be approached with respect to the Fe system, an overall redox equilibrium is not reached as shown by the disagreement between the pe values for the sulfide/sulfate redox pair and the various Fe redox pairs. This is in agreement with previous studies that have shown that an overall redox equilibrium usually does not prevail in the surface geothermal waters neither between the various redox species (Stefánsson et al., 2005) nor for important ligands like sulfur species (Kaasalainen and Stefánsson, 2011). In steam-heated acid waters Fe^{2+}/Fe^{3+} speciation may be controlled by the source (e.g. rock dissolution), Fe(II) oxidation kinetics or microbial reactions. That Fe redox speciation may not have been reached in steam-heated acid waters is in good agreement with the previous findings that Fe concentrations in steam-heated acid water are dominated by rock dissolution (Kaasalainen and Stefánsson, 2012), the slow kinetics of Fe^{2+} oxidation at pH < 4 and observations on the Fe^{2+} oxidizing microorganisms found in acid geothermal water in Iceland (Pétursdóttir et al., 2007, 2008).

Assuming an overall redox equilibrium based on the various pe-values estimated from the reactions (1), (4), (5) and (6) (Fig. 8), the speciation of Fe can be calculated from the Fe_{total} concentrations corresponding to the sum of the Fe(II) and Fe(III) concentrations determined in this study. The results of these calculations are presented in Fig. 9, showing the observed and predicted Fe(II) and Fe(III) concentrations. Even relatively small deviations mean large differences in absolute concentrations (note the logarithmic scale).

5. Summary and conclusions

The chemistry of Fe(II) and Fe(III) was studied in natural geothermal waters from warm and hot springs and pools and sub-boiling wells from active high-temperature geothermal systems in SW Iceland. In order to minimize post-sampling changes in the Fe(II) and Fe(III) concentrations, the determination of Fe(II) and Fe(III) was carried out promptly after sampling using a field-deployed ion chromatography spectrophotometry method. The sampled waters varied widely with respect to the water pH (2.46–9.75), discharge temperature (up to 100 °C) and total dissolved Fe and major ion concentrations. The Fe(II) and Fe(III) concentrations in natural geothermal water (< 0.2 μm fraction) range from < 0.15 to 136 μmoL/L and from < 0.1 to 100 μmoL/L, respectively. An additional determination of Fe(II) and Fe (III) in < 10 kDa and < 1 kDa size fractions suggest that in some cases part of the iron determined in the water from standard filtration may be derived from filter-passing nanosized particles, and thus Fe concentrations in samples fractions collected using standard filtration techniques may not be representative of the truly dissolved Fe concentration. More detailed study on the occurrence of colloidal/nanosized Fe in various types of geothermal waters is a matter of further research. The absolute and relative distribution of Fe(II) and Fe(III) is influenced by the water pH that reflects the water type and the various processes resulting in their formation. In water with a pH of 7–9, the total Fe concentrations are < 2 μmoL/L with Fe(III) predominating. With decreasing pH, the total Fe concentration increases with Fe(II) becoming increasingly important and predominating at pH < 3. In particular at pH ~6 and above, iron redox equilibrium may be approached with Fe(II) and Fe (III) possibly being controlled by equilibrium with respect to Fe minerals, whereas in many acid waters, the Fe(II)/Fe(III) distribution appears to not have reached equilibrium and may be controlled by the

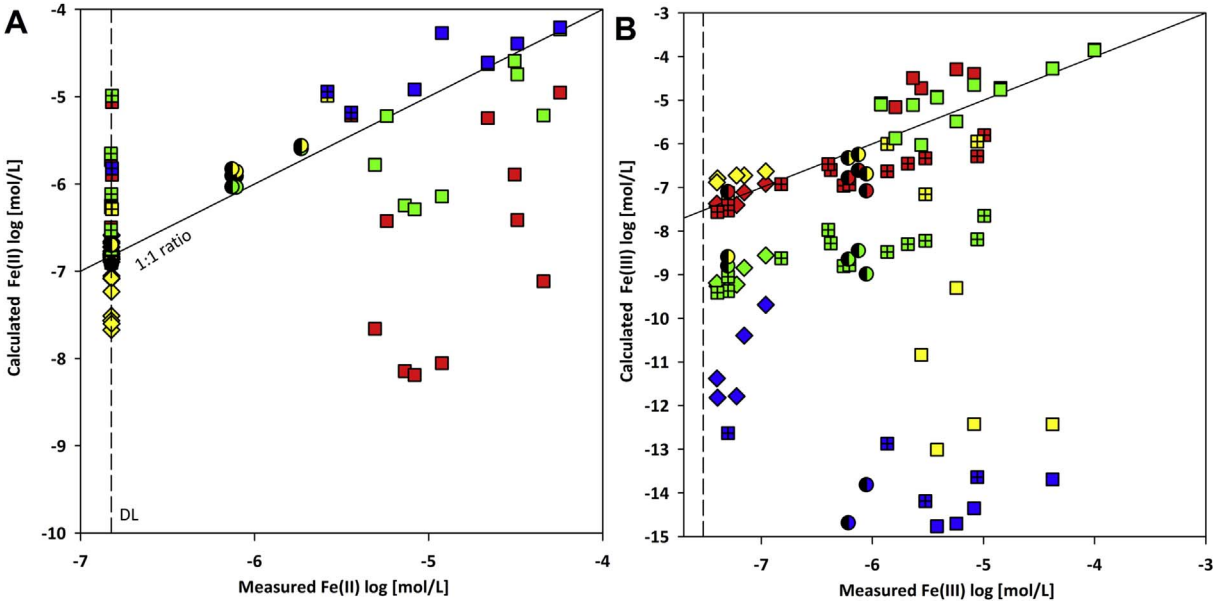

Fig. 9. Comparison of measured **(A)** Fe(II) and **(B)** Fe(III) concentrations to those calculated using the sum of the measured Fe(II) and Fe(III) concentrations and assuming an overall redox equilibrium based on the pe-values for the various redox pairs Fe^{2+}/amorphous-Fe(III)-hydroxide, Fe^{2+}/6-line-ferrihydrite, mackinawite/Fe^{3+}, and H_2S/SO_4, according to reactions (1) and (4)–(6) (section 4.5). In both A and B, the value of the detection limit was used for samples with Fe(II) concentrations below the detection limit, thus representing the maximum Fe(II) present and the minimum estimate of the respective pe-value in the samples. Symbols are according to Fig. 8.

source, reaction kinetics or microbial reactions.

Acknowledgements

This study was funded by the Icelandic Research Fund grant number 120250, and the Energy Research Fund of Landsvirkjun Energy Company. The authors wish to thank Dr. Iwona M. Galezcka, Dr. Nicole Keller and Dr. Snorri Gudbrandsson for their help in the field and the laboratory. The Environment Agency of Iceland and Hotel Geysir are thanked for their collaboration and permission during the field work in the Geysir area.

References

Ármannsson, H., 2016. The fluid chemistry of Icelandic high-temperature geothermal areas. Appl. Geochem. 66, 14–64.
Arnórsson, S., 1969. A Geochemical Study of Selected Elements in Thermal Waters of Iceland. Unpubl. Ph.D. Thesis. Univ. London U.K., pp. 353.
Arnórsson, S., Björnsson, A., Gíslason, G., Gudmundsson, G., 1975. Systematic exploration of the Krísuvík high-temperature area, Reykjanes-peninsula, Iceland. In: 2nd United Nations Symposium on the Development and Use of Geothermal Resources, San Francisco, USA, Icelandic National Energy Authority (Orkustofnun) Report OSJHD 7528, Reykjavik, Iceland (1975).
Arnórsson, S., 1985. The use of mixing models and chemical geothermometers for estimating underground temperatures in geothermal systems. J. Volcanol. Geotherm. Res. 23, 299–335.
Arnórsson, S., 1987. Gas chemistry of the Krýsuvík geothermal field, Iceland, with special reference to evaluation of steam condensation in upflow zones. Jökull 37, 31–47.
Arnórsson, S., Andrésdóttir, A., 1995. Processes controlling the distribution of boron and chlorine in natural waters in Iceland. Geochim. Cosmochim. Acta 59, 4125–4146.
Arnórsson, S., Bjarnason, J.Ö., Giroud, N., Gunnarsson, I., Stefánsson, A., 2006. Sampling and analysis of geothermal fluids. Geofluids 6, 203–216.
Arnórsson, S., Stefánsson, A., Bjarnason, J.Ö., 2007. Fluid-fluid interactions in geothermal systems. Rev. Mineral. Geochem. 65, 259–312.
Ball, J.W., Nordstrom, D.K., 1991. WATEQ4F — User's Manual with Revised Thermodynamic Data Base and Test Cases for Calculating Speciation of Major, Trace and Redox Elements in Natural Waters. USGS Open-File Report. pp. 91–183.
Banfield, J.F., Navrotsky, A., 2001. Nanoparticles and the Environment. Mineralogical Society of America.
Batley, G.E., 1989. Trace Element Speciation - Analytical Methods and Problems. CRC Press.
Benning, L.G., Wilkin, R.T., Barnes, H.L., 2000. Reaction pathways in the Fe-S system below 100°C. Chem. Geol. 167, 25–51.
Björke, J., Stefánsson, A., Arnórsson, S., 2015. Surface water chemistry at Torfajökull, Iceland—quantification of boiling, mixing, oxidation and water–rock interaction and reconstruction of reservoir fluid composition. Geothermics 58, 75–86.
Butler, I.B., Böttcher, M.E., Rickard, D., Oldroyd, A., 2004. Sulfur isotope partitioning during experimental formation of pyrite via the polysulfide and hydrogen sulfide pathways: implications for the interpretation of sedimentary and hydrothermal pyrite isotope records. Earth Planet Sci. Lett. 228, 495–509.
Cornell, R.M., Schwertmann, U., 2003. The Iron Oxides. Structure, Properties, Reactions, Occurrences and Uses, second ed. Wiley.
Eaton, A.D., Clesceri, L.S., Rice, E.W., Greenberg, A.E. (Eds.), 2005. Standard Methods for the Examination of Water and Wastewater, twenty-first ed. American Public Health Association, American Water Works Association and Water Environment Federation.
Fox, L.E., 1988. The solubility of colloidal ferric hydroxide and its relevance to iron concentrations in rivers. Geochim. Cosmochim. Acta 52, 771–777.
Gilbert, B., Lu, G., Kim, C.S., 2007. Stable cluster formation in aqueous suspensions of iron oxyhydroxide nanoparticles. J. Colloid Interface Sci. 313, 152–159.
Gunnlaugsson, E., Arnórsson, S., 1982. The chemistry of iron in geothermal systems in Iceland. J. Volcanol. Geotherm. Res. 14, 281–299.
Hardardóttir, V., Brown, K.L., Fridriksson, T., Hedenquist, J.W., Hannington, M.D., Thorhallsson, S., 2009. Metals in deep liquid of the Reykjanes geothermal system, southwest Iceland: implications for the composition of seafloor black smoker fluids. Geology 37, 1103–1106.
Heinrich, C.A., Seward, T.M., 1990. A spectrophotometric study of aqueous iron (II) chloride complexing from 25 to 200°C. Geochim. Cosmochim. Acta 54, 2207–2221.
Hiemstra, T., 2015. Formation, stability, and solubility of metal oxide nanoparticles: surface entropy, enthalpy, and free energy of ferrihydrite. Geochim. Cosmochim. Acta 158, 179–198.
Jónsson, J., 1978. Geological Map of the Reykjanes Peninsula. Reykjavik Energy Authority Report OS-JHD-7831.
Kaasalainen, H., Stefánsson, A., 2011. Sulfur speciation in natural hydrothermal waters. Icel. Geochim. Cosmochim. Acta 75, 2777–2791.
Kaasalainen, H., Stefánsson, A., 2012. The chemistry of trace elements in surface geothermal waters and steam. Icel. Chem. Geol. 330–331, 60–85.
Kaasalainen, H., Stefánsson, A., Giroud, N., Arnórsson, S., 2015. The geochemistry of trace elements in geothermal fluids. Icel. Appl. Geochem 62, 207–223.
Kaasalainen, H., Stefánsson, A., Druschel, G., 2016. Determination of Fe(II), Fe(III) and Fetotal in geothermal water by IC-Vis spectrophotometry. Int. J. Environ. Anal. Chem. 96, 1074–1090.
Kappler, A., Straub, K., 2005. Geomicrobiological cycling of iron. Rev. Mineral. 59, 85–108.
Konhauser, K.O., Ferris, F.G., 1996. Diversity of iron and silica precipitation by microbial mats in hydrothermal waters, Iceland: implications for Precambrian iron formations. Geology 24, 323–326.
Majzlan, J., Navrostky, A., Schwertmann, U., 2004. Thermodynamics of iron oxides: Part III. Enthalpy of formation and stability of ferrihydrite (~$Fe(OH)_3$), schwertmannite (~$FeO(OH)_{3/4}(SO_4)_{1/8}$, and ε-$Fe_2O_3$. Geochim. Cosmochim. Acta 68, 1049–1059.
Markússon, S.H., Stefánsson, A., 2011. Geothermal surface alteration of basalts, Krýsuvík Iceland – alteration mineralogy, water chemistry and the effects of acid supply on the alteration process. J. Volcanol. Geotherm. Res. 206, 46–59.
McCleskey, R.B., Chiu, R.B., Nordstrom, D.K., Campbell, K.M., Roth, D.A., Ball, J.W., Plowman, T.I., 2014. Water-chemistry Data for Selected Springs, Geysers, and Streams in Yellowstone National Park, Wyoming. Beginning 2009. US Geological Survey. .
Nordstrom, D.K., Ball, J.W., McCleskey, R.B., 2005. Ground water to surface water:

chemistry of thermal outflows in Yellowstone National Park. In: Inskeep, W., McDermott, T.R. (Eds.), Geothermal Biology and Geochemistry in Yellowstone National Park. Montana State University, pp. 73–94.
Nordstrom, D.K., Plummer, L.N., Langmuir, D., Busenberg, E., May, H.M., Jones, B.F., Parkhurst, D.L., 1990. Revised chemical equilibrium data for major water-mineral reactions and their limitations. In: Melchior, D.C., Bassett, R.L. (Eds.), Chemical Modeling in Aqueous Systems II. A.C.S. Symposium Series 416, pp. 398–413.
Parkhurst, D.L., Appelo, C.A.J., 1999. User's Guide to PHREEQC (Version 2) — a Computer Program for Speciation, Batch-reaction, One-dimensional Transport, and Inverse Geochemical Calculations. Water Resources Investigations Report (United States Geological Survey). pp. 99–4259.
Pétursdóttir, S., Björnsdóttir, S., Ólafsdóttir, S., Hreggvidsson, G.Ò., 2008. Lífræðilegur Fjöbreytileiki Í Hverum Að Theistreykjum Og Í Gjástykki. Matís Ltd Reports 39-08. pp. 65 (in Icelandic).
Pétursdóttir, S., Òlafsdóttir, S., Magnúsdóttir, S., Hreggvidsson, G.Ò., 2007. Lífríki Í Hverum Í Krýsuvik Og Gunnuhver Á Reykjanesi. Matís Ltd Reports 31-07. pp. 33 (in Icelandic).
Pokrovsky, O.S., Schott, J., 2002. Iron colloids/organic matter associated transport of major and trace elements in small boreal rivers and their estuaries (NW Russia). Chem. Geol. 190, 141–179.
Pope, J., Brown, K.L., 2014. Geochemistry of discharge at Waiotapu geothermal area, New Zealand – trace elements and temporal changes. Geothermics 51, 253–269.
Rickard, D., Luther III, G.W., 1997. Kinetics of pyrite formation by the H2S oxidation of iron(II) monosulfide in aqueous solutions between 25 and 125°C: the mechanism. Geochim. Cosmochim. Acta 61, 135–147.
Rue, E.L., Bruland, W., 1995. Complexation of iron(III) by natural organic-ligands in the central North Pacific as determined by a new competitive ligand equilibration adsorptive cathodic stripping voltammetric method. Mar. Chem. 50, 117–138.
Schoonen, M.A.A., Barnes, H.L., 1991. Reactions forming pyrite and marcasite from FeS precursors below 100 °C. Geochim. Cosmochim. Acta 55, 1505–1514.
Shock, E.L., Holland, M., Meyer-Dombard, D., Amend, J.P., Osburn, G.R., Fischer, T.P., 2010. Quantifying inorganic sources of geochemical energy in hydrothermal ecosystems, Yellowstone National Park, USA. Geochim. Cosmochim. Acta 74, 4005–4043.
Stefánsson, A., 2007. Iron hydrolysis and solubility a 25°C. Environ. Sci. Technol. 41, 6117–6123.
Stefánsson, A., Arnórsson, S., 2002. Gas pressures and redox reactions in geothermal fluids in Iceland. Chem. Geol. 190, 251–271.
Stefánsson, A., Amórsson, S., Sveinbjörnsdóttir, A.E., 2005. Redox reactions and potentials in natural waters at disequilibrium. Chem. Geol. 221, 289–311.
Stefánsson, A., Gíslason, S.R., Arnórsson, S., 2001. Dissolution of primary minerals in natural waters II. Mineral saturation state. Chem. Geol. 172, 251–276.
Stefánsson, A., Gunnarsson, I., Giroud, N., 2007. New methods for the direct determination of dissolved inorganic, organic and total carbon in natural waters by Reagent-Free™ Ion Chromatography and inductively coupled plasma atomic emission spectrometry. Anal. Chim. Acta 582, 69–74.
Stefánsson, A., Keller, N.S., Gunnarsson Robin, J., Kaasalainen, H., Björnsdóttir, S., Pétursdóttir, S., Jóhannesson, H., Hreggvidsson, G.Ó., 2016. Quantifying mixing, boiling, degassing, oxidation and reactivity of thermal waters at Vonarskard. Icel. J. Volcanol. Geotherm. Res. 309, 53–62.
Steingrímsson, B., Tulinius, H., Franzson, H., Sigurdsson, Ó., Gunnlaugsson, E., Gunnarsson, G., 1997. Ölkelduháls, Well ÖJ-1, Drilling, Exploration and Production Characteristics. Final report. Orkustofnun, Reykjavík, report OS-97019 (in Icelandic). pp. 190.
Steinthórsson, S., Sveinbjörnsdóttir, A.E., 1981. Opaque minerals in geothermal well No.7 Krafla. North. Icel. J. Volcanol. Geotherm. Res. 10, 245–261.
Stumm, W., Morgan, W., 1981. Aquatic Chemistry – an Introduction Emphasizing Chemical Equilibria in Natural Waters, second ed. John Wiley and Sons.
Stumm, W., Sulzberger, B., 1992. The cycling of iron in natural environments: considerations based on laboratory studies on heterogeneous redox processes. Geochim. Cosmochim. Acta 56, 3233–3257.
Tobler, D.L., Benning, L., 2011. Bacterial diversity in five Icelandic geothermal waters: temperature and sinter growth rate effects. Extremophiles 15, 473–485.
Tobler, D.J., Stefánsson, A., Benning, L.G., 2008. In-situ grown silica sinters in Icelandic geothermal areas. Geobiology 6, 481–502.